A DEEP LEARNING APPROACH TO RAPID REGIONAL POST EVENT SEISMIC DAMAGE ASSESSMENT

Y. J. Xu[(1)], X. Z. Lu[(2)], Y. Tian[(3)], E. Taciroglu[(4)]

[(1)] *PhD candidate, Department of Civil Engineering, Tsinghua University, xuyongjia0904@163.com*
[(2)] *Professor, Department of Civil Engineering, Tsinghua University, luxz@tsinghua.edu.cn*
[(3)] *PhD, Department of Civil Engineering, Tsinghua University, t-y14@tsinghua.org.cn*
[(4)] *Professor, Department of Civil & Env. Engineering, University of California, Los Angeles, etacir@g.ucla.edu*

Abstract

Earthquakes have caused severe economic losses and casualties around the world. Once an earthquake occurs, timely and accurate evaluation of the seismic damage in a disaster area is of great importance for organizing effective post-event relief. However, conventional in-situ inspection methods are time-consuming and labor intensive. Thus, they are unlikely to meet the requirements of proper emergency response when deployed alone. Although post-event damage/loss prediction methods that are based on fragility analyses are efficient, their accuracy and universality have not yet been established. A more accurate, yet less computationally efficient, approach is to use recorded ground motions in nonlinear time-history analyses (NLTHA) of structure-specific predictive models. However, carrying out such complicated NLTHA on structure-by-structure basis across an entire urban region is not yet quite possible to meet the granular demands of emergency response efforts. Given this perspective, a rapid regional post-event seismic damage assessment method based on convolutional neural network (CNN) is proposed in this study, which offers fair accuracy and can render predictions in real-time. In this approach, an inventory of buildings in a given region, the definitions of their damage/performance levels, and a suite of anticipated ground motions for the region are established. These data are then used in NLTHA to establish a training set for CNN that will estimate the damage state of a building or selected region, given the time-frequency distribution (TFD) graphs of a ground motion. This CNN estimate can be made nearly instantaneously—i.e., it is suitable for rapid post-event assessment—and can provide high accuracy provided that the training set is rich. CNN is particularly well suited for this task because TFDs are essentially visual representations of both the frequency-domain features, and instantaneous as well as cumulative time-domain features of ground motions. The proposed methodology is verified with a numerical case study on the 3-story special moment frame building.

Key words: seismic damage prediction; real-time; convolutional neural network (CNN); time-frequency distribution

1. Introduction

Earthquakes have caused severe economic losses and casualties in many countries. Once an earthquake occurs, organizing effective post-disaster response is a key factor in reducing economic losses and casualties. Therefore, it is necessary to evaluate the seismic damage in the disaster area timely and objectively. This task bears strict and high demands on the accuracy and expediency of seismic damage predictions. A delayed or inaccurate prediction may result in catastrophic consequences [1].

Because site investigations of seismic damage are time-consuming and require well-trained professionals, they cannot meet emergency response requirements. To solve this problem, several near real-time seismic damage evaluation systems have been established, including PAGER [2], GDACS [3], etc. These systems acquire information about the earthquake from sensor networks, and the corresponding seismic damage is evaluated through fragility analysis. The economic losses and casualties are then assessed by using empirical loss models calibrated with historical earthquake events.

Post-event seismic damage assessment methods based on the nonlinear time-history analysis (NLTHA) with a regional inventory of structural models have also been proposed in recent years. For example, Lu and Guan [4] proposed a city-scale approach based on NLTHA and developed the RED-ACT system [5]. The RED-ACT system acquires real-time ground motions through existing strong motion networks and comprehensively evaluates the seismic damage by conducting NLTHA on typical individual buildings and target regions. The accuracy of the method has been explored and verified in many aspects in prior studies [6, 7]. It has also been adopted by the SimCenter project supported by the US National Science Foundation [8] and the emergency response processes of several earthquakes [5].

It is possible to generalize the aforementioned efforts on rapid post-event seismic damage assessment method. The basic steps of a generic and generalized rapid seismic damage assessment method appear to be the following: (1) Establish a database of ground motions and an available inventory of building analysis models. For data-driven methods, it's also necessary to analyze the seismic damage on buildings caused by these ground motions. (2) Establish mapping rules between the applied ground motions and the predicted seismic damages. (3) Once a new earthquake occurs, use these pre-established mapping rules and rapidly estimate (in near real-time) the seismic damage, given the information of new earthquake events.

All of the previously mentioned—namely, NLTHA-, fragility-based—approaches are clearly a sub-class of this broader definition. The key issue is to identify and employ an accurate and computationally efficient mapping between the excitation and the structural damage. In this regard, NLTHA-based methods lie at one end of the spectrum. The NLTHA-based methods take in the entire time series of recorded excitations as input, which, if correctly used, always produce highly accurate predictions of the actual damage [9, 10]. However, at the present time, they cannot yet meet the near real-time requirements of emergency response efforts at a regional-scale or city-scale, even with large computational resources [4, 11].

At the other end of the spectrum lie the fragility-based approaches. These post-event assessment tools are clearly far more efficient than the NLTHA-based approaches. However, existing studies have shown that many of the commonly used 1D scalar ground motion features cannot alone predict the seismic damage well, including magnitude, peak ground acceleration or velocity (PGA or PGV), spectral acceleration at fundamental period, significant duration, etc. (e.g., [7, 12]). While more advanced fragility analysis based on vector-valued intensity measures are being devised (e.g., [13, 14]), seismic fragilities that are based only on a limited number of input ground motion attributes will unlikely produce uniformly accurate predictions. Besides, for areas lacking historical earthquake data, existing empirical fragility models may not be applicable.

Given the observations and perspectives provided above, it appears necessary to devise methods that can produce results nearly as quickly as the fragility-based methods, but at higher accuracy levels, ideally approaching those afforded by structure specific NLTHA-based regional rapid post-event assessment. In order to achieve this feat, it is necessary to devise a method that explicitly or implicitly takes into account complex ground motion features, and rapidly maps them into response/damage/loss measures.

Ground motion features can be first divided into two basic categories—namely, time- and frequency-domain features. Correlations of a variety of these features under both categories with specific performance/damage measures continue to be examined for common structural systems [15]. One pathway towards combing these complex features goes through the use of time-frequency distributions (TFDs) [16] of ground motions. Existing studies have explored the utilization of TFDs of ground motion records, which mainly focus on the structural monitoring and identification studies (for earliest examples, see [17, 18]).

Among many alternatives, the "wavelet transform" [19] yields an optimal TFD of the input signal. TFDs obtained through a continuous wavelet transform comprehensively embodies both the time- and the frequency-domain features of the ground motion signals. Illustrated through the example graph shown in Figure 1, each data point in a TFD graph corresponds to a certain time (horizontal axis) and frequency component (vertical axis), the color of which represents the absolute value (magnitude) of the wavelet coefficient. However, the data embedded in such a plot is complex, outside of the few examples discussed above, have not been used in structural performance or damage assessment previously. Nevertheless, it appears possible to establish useful mapping rules between such TFD data and structural response, as will be described next.

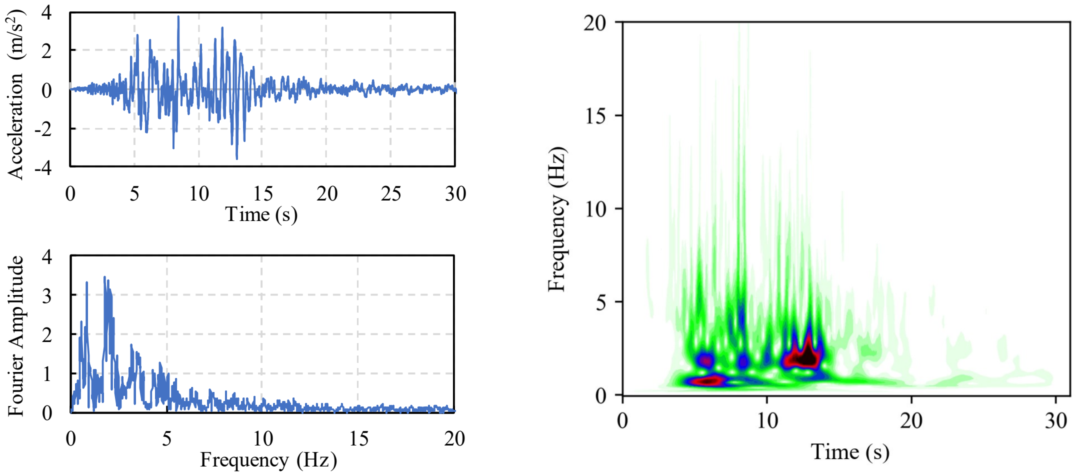

(a) Time series and Fourier amplitude (b) Time-frequency distribution (TFD) graph

Figure 1 – Different ways to represent a ground motion

In recent years, neural network technology has developed rapidly, and recorded significant accomplishments in nonlinear and fuzzy learning tasks [20]. Among the many types of neural networks, convolutional neural network (CNN) emerged as an important algorithm in the field of computer vision, and has been widely used in image recognition, video processing, autonomous navigation applications, etc. In the field of earthquake engineering, CNN is also recognized. For example, Vetrivel et al. [21], Xiong et al. [22] identified CNN as a potentially highly useful tool in post-disaster damage identification.

These prior studies suggest that it should be possible to use CNN to establish accurate mappings between TFDs and structural response/damage. While the training, calibrating, and validating a CNN will be time-consuming, a trained CNN can yield real-time predictions with high-accuracy after an earthquake. During an actual event, the only computation needed will be the conversion of recorded signals into TFD and supplying them to the pre-trained CNN. These calculations are highly scalable in terms of parallel computation, as each record can be processed by a dedicated processor; and more importantly, the continuous wavelet transform of an individual time series signal can be rapidly carried out. In what follows, such a CNN-based rapid post-event seismic damage prediction methodology is devised and examined in terms of both accuracy and efficiency.

2. Framework

The framework of the proposed rapid CNN-based post-event seismic damage assessment method is shown in Figure 2. Developing and applying this method comprises three phases: (1) Establish an inventory of predictive models of the target buildings, along with a suite of ground motions (ideally representatives of ground motions expected for the particular region that building inventory is located at). Carry out NLTHA with each model and each ground motion and obtain damage states from such calculations. (2) Establish the mapping rules between the computed damage states and ground motions. The TFD of each ground motion and the resulting damage are input-output training pairs for CNN. Select CNN models with outstanding predictive abilities. (3) During emergency responses, obtain the TFD of each recorded (or estimated) motion and use the pre-trained CNN to estimate the seismic damage.

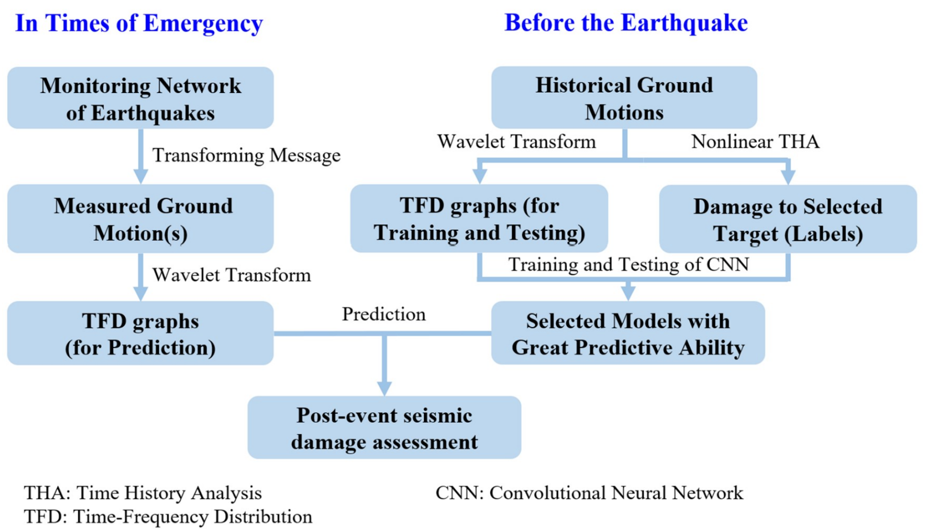

Figure 2 – Framework of the proposed CNN method

It is clear that depending on the resolution/granularity of the ground motion measurements and the details of the model inventory, different variants of the general method described above can be generated. For example, ground motions can be estimated at locations that lack measurement stations, and building models can be coarsely generated based on some coarse metadata that describes the region by an appropriate algorithm for refined predictions [6]—albeit with larger uncertainty compared to the ideal scenario wherein ground motions are sampled with spatially dense sensor arrays, and every building in the region is individually modeled. Alternatively, both the ground motion records and building models can be lumped together (e.g., by city blocks) for coarser predictions.

2.1 Establishing datasets

At present, there are several open-access ground motion databases such as the PEER NGA-East/West/West2 database [23] of the United States, and the K-NET database [24] of Japan that can be used for the task at hand. For the present effort, 10,548 ground motions are obtained from the PEER NGA-West database. To generate the corresponding TFD graphs, the ground motion records are pre-processed and continuous wavelet transformed (details of these procedures are provided later).

The damage states of the target buildings are obtained through conventional or city-scale NLTHA [4] using the obtained ground motions. The damage state of a building is divided into five different levels—namely, “none damage”, “slight damage”, “moderate damage”, “extensive damage”, and “complete damage”. These rather-qualitative damage classifications are linked to specific structural response/damage states in various guideline documents (e.g., [25, 26]), which are also adopted in this study.

Note that it would be better to select proper ground motion datasets for the training according to the specific situations of the selected building. For example, if the selected building is close to a subduction fault, the CNN models trained by ground motions with similar source characteristics are likely to have better performance. As such, the subsequent development in the remainder of this study should be viewed as an example, rather than an all-encompassing solution.

2.2 Training and testing of CNN

The training and testing of CNN are carried out using the TFDs and damage indicators of ground motions. The CNN models with outstanding predictive ability are then selected. To ensure independence between the training and testing datasets, another 1,875 ground motions obtained from the K-NET database [24] are chosen as the testing dataset in the present study (details of these procedures are provided later).

The proposed method is demonstrated using one typical building in this study, which is a 3-story special moment reinforced concrete (RC) frame with a height of 10 meters. The seismic design intensity of it is degree VII (with a PGA of 0.10g at a 10% probability of exceedance in 50 years). In this one-building case study, the accuracy of CNN predictions, training and prediction efficiency, along with the influences of different CNN network structures and hyperparameters are examined.

2.3 Seismic damage prediction

At present, several real-time earthquake monitoring networks have been established, such as the K-NET of Japan [24] and the strong motion network of China [27]. Once an earthquake occurs, these networks can record the ground motions and transmit them real time. After receiving the measured ground motions, the wavelet transform will be carried out automatically to generate the corresponding TFDs. With these TFD graphs, the preloaded CNN models can predict the damage states of the target buildings or regions immediately. It should be emphasized that if the CNN are properly trained, there is no need to conduct the training and testing again in times of emergency.

3. Seismic damage prediction based on CNN

3.1 Obtaining and Pre-processing of samples

3.1.1 Training Samples

In the present study, 10,548 ground motions are obtained from the PEER NGA-West database [23]. After the pre-processing, 42,192 samples are obatined and randomly divided into two sets—namely, the training set (95%), and the validation set (5%). The pre-processing is conducted under the following steps.

Step 1. Amplitude scaling: Destructive earthquakes are inherently less frequent. Moreover, the proportion of strong near-field ground motions among all records of a destructive earthquake is small. Therefore, only limited ground motion records will result in moderate or more severe damage states. To remedy this issue (of the inherent rareness of high-amplitude motions in the record inventory), amplitude-scaling is utilized in the present study.

Existing studies have proved that applications of excessively large scaling factors on recorded ground motions may result in significant errors; and scaling factors less than 4.0 are typically deemed acceptable [28-30]. Therefore, scaling factors in this study are selected as 1.0, 2.0, 3.0, and 4.0. By multiplying each ground motion with these scaling factors, 42,192 amplified ground motions are generated. It can be seen from Table 1 that the proportion of ground motions that will produce moderate or more severe damage outcomes is increased by 3.62 times after this amplification; and as such, the diversity of the samples is enhanced.

Table 1 – The proportions of ground motions resulting with different damage states

Damage state	None	Slight	Moderate	Extensive	Complete

Before the amplification	62.68%	32.44%	4.29%	0.53%	0.06%
After the amplification	39.13%	43.22%	13.16%	2.91%	1.58%

Step 2. Adjustment of duration: Before the generation of TFD graphs, it's necessary to make the durations of all ground motions uniform. Otherwise, the same point on each graph will have different meanings. Considering that most urban buildings do not exceed 30 floors. The fundamental periods of buildings can be estimated with the simple Equation (1) [31]:

$$T_1 = 0.1N \tag{1}$$

where T_1 is the fundamental period, and N is the number of floors. Together with the assumption adopted on building heights, the fundamental periods of most urban buildings are less than 3 s.

Again, following the Code for Seismic Design of Buildings (GB 50011-2010) in China [32], the durations of ground motions used for NLTHA should be no less than 5 to 10 times of the fundamental periods of the target building. Consequently, a 30-sec ground motion duration is sufficient. As such, the durations of all ground motions are modified to 30 s. Only the acceleration data from 15 s before to 15 s after the occurrence of the PGA are retained.

The aforementioned tailoring of the ground motions is only carried out for generating the TFD graphs, whereas ground motions without any duration adjustment are used for calculating damage states using NLTHA. As such, the labels of the samples are not influenced by the adjustments of duration. The mapping rules established via CNN are still between the ground motions and the real damage states, and no systematic bias is created due to duration adjustments.

Step 3. Generation of TFD graphs: Continuous wavelet transforms are performed on all processed ground motions, and the absolute values of the wavelet coefficients are calculated for each time and frequency coordinate. The continuous wavelet transform is performed using the "Complex Gaussian wavelet 8 (cgau8)" that is available through the Python library named "PyWavelets" [33]. Subsequently, the Python library "Matplotlib" is used for generating the TFD graphs from wavelet amplitude data. The horizontal axes (time) of all figures range from 0 to 30 s (per the duration adjustment described above). The vertical axes (frequency) range from 0 Hz to 20 Hz, which is deemed appropriate for most earthquake engineering applications [34, 35].

Step 4. Cropping of the TFD graphs: To avoid the interference of axes and labels on the training process of CNN, all figures are cropped so that only the TFD data is visible to the CNN.

3.1.2 Testing Samples

To guarantee the independence between the training and testing datasets, testing samples are obtained from the K-NET database [24] of Japan. Ground motions satisfying the following requirements are used first: (1) Motions recorded from January 2011 to January 2019; (2) Motions recorded during earthquakes of magnitude 6.0 or above. Since all ground motions from the PEER NGA-West database are recorded during or before 2008 [23], there are no duplicate records within the training or testing sets. To ensure that the testing set is rich, 1,875 ground motions are chosen as testing samples from the following two categories: (1) All ground motions whose PGA are larger than 1 m/s^2 (1,246 records in total); and (2) 10% of the ground motions (randomly selected) whose PGAs lie in the range of 0.2 m/s^2 to 1 m/s^2 (629 records in total)

The prediction accuracy of the testing set is adopted as the key indicator of the performance of the proposed CNN method. To this end, the amplitude scaling is not carried out on testing samples in order to minimize the noise or other errors, but the remaining steps of pre-processing (duration adjustment, generation and cropping of TFD graphs) are still carried out for the testing set.

3.2 Establishment of CNN and prediction results

CNN is a powerful tool for processing image data. The typical structure of CNN includes input, output, and multiple hidden layers [36]. In the present application, the input layer receives the TFD graphs, and the output layer provides the prediction of the damage state of the building for which the CNN is trained. The hidden layers are complex, which always include convolutional, pooling, activation, and classification layers. In addition, CNN is likely to contain other kinds of layers, such as dropout, flatten, and dense layers. Specific functions of these layers have already been illustrated in existing sources (e.g., [37]).

"TensorFlow" [38] is an efficient and convenient platform in the field of machine learning. Here, a CNN containing 18 hidden layers is devised as the reference network based on TensorFlow. The structure of this reference network is shown in Figure 3. The sizes of convolution and maximum pooling kernels are selected as 3×3 and 2×2, respectively. The activation function is "ReLU". Other important settings are shown in Table 2.

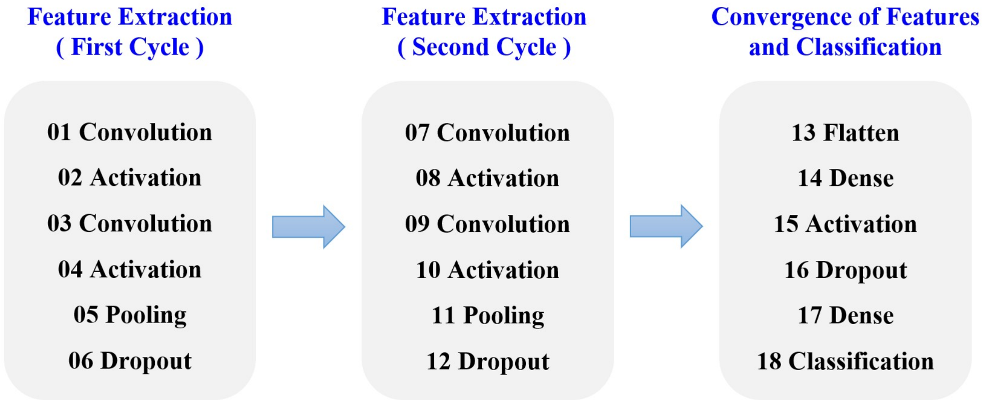

Figure 3 – The structure of the reference network

The stochastic gradient descent (SGD) method is selected for optimizing the reference network; and the "momentum" algorithm is utilized to accelerate convergence [39]. The indicator of "loss" is chosen as "categorical cross entropy" [40], which is commonly used for classification tasks.

To examine the impact of network structures on the predictive ability and training efficiency, sensitivity studies are carried out on the reference network, as shown in Table 2. Additionally, to verify the rationality of the selected input dimension (sizes of figures, 64 pixels × 64 pixels in this study), another four networks are established as the control group. The structures and hyperparameters of these four networks are the same as Networks 1, 2, 3, and 5 in Table 2. However, the input dimension (size of figures) is 128 × 128. Training of all networks is carried out and the acquired CNN models are tested on the testing set. The prediction accuracy and consumed time of the training process are shown in Table 3. Each network is trained three times to eliminate the influence of random factors such as the initialization of networks. The maximum prediction accuracy among three training cases is recorded each time.

The following conclusions can be drawn from Table 3:

(1) The proposed CNN method can predict the damage states of the target building caused by ground motions well. The highest accuracy on the testing set is up to 92.64%.

(2) Networks 3 and 4 have higher predictive ability and are efficient overall. Therefore, these networks are suitable for implementing the seismic damage prediction task. The predictive ability of simpler networks (such as Networks 1 and 2) is relatively low. Meanwhile, there are more complex networks like Networks 5 and 6 that require more than 24 hours for training, which offer no significant advantage in terms of accuracy.

(3) The complexity of the network within a reasonable range is not the controlling factor of accuracy.

(4) Compared to larger input dimension of 128 × 128, CNN with input dimension of 64 × 64 can save 70.42% of training time on average; and its prediction accuracy is approximately the same (CNN with 64 × 64 input dimension is 1.56% higher on average).

Table 2 – Adjustments of network structures and values of important hyperparameters

No.	Adjustments of network structure (Compared with the reference network)	Number of hidden layers	Values of important hyperparameters
1	Removing hidden layers 3, 4, 9 and 10	14	Dropout ratio: 0.30 Learning rate: 0.0100 Input dimension: 64 × 64 Batch size: 50 Maximum iterations: 30
2	Removing hidden layers 3 and 4	16	
3	Reference network	18	
4	Copying layers 7 and 8, inserting them between layers 10 and 11	20	
5	Copying layers 1 and 2, inserting them between layers 4 and 5	20	
6	Copying layers (1, 2) and (7, 8), inserting them between layers (4, 5) and (10, 11), respectively	22	

Table 3 – Consumed time and prediction accuracy of different networks

No.	Number of hidden layers	Experimental group (Input dimension: 64 × 64)		Control group (Input dimension: 128 × 128)	
		Accuracy (%)	Time (h)	Accuracy (%)	Time (h)
1	14	88.0	8.9	87.5	36.1
2	16	88.8	12.6	90.7	47.9
3	18	92.6	18.9	87.5	61.5
4	20	91.5	22.3	-	-
5	20	91.3	26.6	88.6	72.5
6	22	91.6	29.2	-	-

4. Detailed analysis

4.1 Sensitivity studies on hyperparameters

"Dropout ratio" and "Learning rate" are two important hyperparameters for CNN, which may affect the predictive ability and the training efficiency of networks. The dropout ratio mainly influences the generalization ability of the network, which enables the network to avoid overfitting somehow and has been widely recognized in existing studies [41, 42]. Learning rate is also an important hyperparameter which affects the updating of networks. Using a higher learning rate may accelerate the training process. But if this value is excessive, it will be difficult or even impossible for the network to converge because of the repeated fluctuations around the extreme points.

To discuss the impact of dropout ratio on predictive ability, 40 networks with four different structures (Networks 2 to 5 in Table 2) are trained and tested. Srivastava et al. [42] point out that setting the dropout ratio to 0.5 is ideal for avoiding overfitting. However, networks with lower dropout ratios may retain more useful information. Therefore, the values of setting dropout ratio values from 0.05 to 0.50 are examined. Specific values of the dropout ratio and corresponding results are shown in Table 4.

Besides, to explore the influence of learning rate, another 28 networks with four different structures (Networks 2 to 5 in Table 2) are also trained and tested. The values of the learning rate vary from 0.0025 to 0.0175. Specific values of the learning rate and the corresponding results are shown in Table 5.

The following conclusions can be drawn from Tables 4 and 5:

(1) Adjustments of dropout ratio and learning rate do not have a significant influence on the prediction accuracy. Neither hyperparameter is the controlling factor of predictive ability.

(2) For the successful training processes in this study, the accuracy within ten iterations can be quite close to that of the optimal model. The occurrence of the optimal model is delayed when the learning rate is too small (e.g., 0.0025). However, the selection of maximum iterations as 30 times is still sufficient.

Table 4 – Values of the dropout ratio and corresponding results

Dropout ratio	No.	Accuracy (%)	No.	Accuracy (%)	No.	Accuracy (%)	No.	Accuracy (%)
0.05	2	89.3	3	90.7	4	88.6	5	88.5
0.10		89.7		89.1		89.3		89.3
0.15		89.6		89.0		87.1		89.6
0.20		89.2		88.2		87.9		88.4
0.25		88.3		89.9		90.3		92.3
0.30		88.8		92.6		91.5		91.3
0.35		87.7		89.0		90.1		89.6
0.40		86.6		89.1		89.6		88.3
0.45		88.2		88.2		88.1		90.8
0.50		89.4		88.3		89.5		89.3

Note: "No." means the number of network structures as shown in Table 2.

Table 5 – Values of the learning rate and corresponding results

Learning rate	No.	Accuracy (%)	No.	Accuracy (%)	No.	Accuracy (%)	No.	Accuracy (%)
0.0025	2	87.1	3	88.7	4	89.7	5	88.4
0.0050		87.8		89.5		89.2		89.5
0.0075		88.1		89.0		88.3		90.3
0.0100		88.8		92.6		91.5		91.3
0.0125		86.6		88.2		89.3		89.7
0.0150		87.4		89.4		88.9		90.6
0.0175		86.1		88.2		89.3		88.4

In addition, the training process of CNN has a certain probability of failure to completion. 250 more cases are submitted in order to analyze the impact of network structure and learning rate on the failure probability. It can be seen that the more complex the network is, the higher the probability of failure is. In addition, for networks with the same structure, larger learning rate clearly leads to a higher probability of failure and thus reducing the training efficiency. Therefore, the recommended range of learning rate is 0.0050 to 0.0100.

4.2 Analysis of Prediction deviations

The proposed method has outstanding predictive ability and training efficiency. However, although the overall prediction accuracy is high, the deviations on some samples may be unacceptable. Therefore, it should be considered during model selection. After taking the prediction deviations into consideration, four models with the best performances are selected from all the CNN models acquired within 10 iterations and corresponding deviations are analyzed (as shown in Table 6).

It can be seen from Table 6 that the best models can not only predict the damage states of most samples correctly, but also limit the prediction deviations of all the remaining samples within ±1 level. Given that the evaluation of seismic damage level has inherent randomness, the deviations are acceptable to some extent. For example, two RC frames with the maximum inter-story drift ratio (IDR) of 1.99% and 2.01% are identified as “moderate damage” and “extensive damage”, respectively [4]. However, the maximum IDRs only differ by 0.02%, which is quite common and acceptable. Consequently, the proposed method has high prediction accuracy and acceptable deviation. Thus, it is valuable in practical applications.

Table 6 – Detailed information and prediction deviations of selected models

Network Series	Dropout ratio	Learning rate	Proportion of samples with different deviations		
			0 level	±1 level	other
2	0.20	0.0100	88.4%	11.6%	0.0%
3	0.30	0.0125	88.2%	11.8%	0.0%
4	0.05	0.0100	88.6%	11.4%	0.0%
5	0.10	0.0100	89.3%	10.7%	0.0%

4.3 Efficiency of the proposed method

To evaluate the computational efficiency of the proposed method, the consumed time of the CNN models are analyzed. Noting that the training and testing of networks are fully completed before the earthquake, thus they do not influence the prediction efficiency during emergency response.

Ten ground motions are randomly selected from the 1,875 testing samples for the analyzing of the predicting efficiency. A selected CNN model is preloaded on the prediction platform. Once the measured ground motions are transmitted to the prediction platform, the entire process—including pre-processing, data input and predicting—is carried out automatically. All predictions and calculations are conducted on a regular computing workstation (with an “Intel Xeon Gold 6154 @ 3.00 GHz” CPU and no GPU).

The CNN model only takes approximately 0.5s to fulfill the seismic damage prediction of each ground motion (including loading and pre-processing of ground motions). The proposed method is, therefore, much faster than the NLTHA method (e.g., [4, 9, 10]) based on this empirical observation. Considering the high efficiency of the proposed method, together with the fact that the NLTHA requires large-scale computational resources to be readily available, the CNN-based approach appears to be far more amenable for rapid predictions of structural damage.

5. Conclusions

A post-event seismic damage assessment method based on CNN is proposed in this study, which takes the TFD graphs of ground motions as input. Based on the proposed method, real-time seismic damage prediction study on a typical 3-story special moment RC frame is carried out. The best way of constructing a CNN and the selection of the hyperparameters are discussed. The following conclusions can be drawn in this study:

(1) The CNN-based method has an acceptable prediction accuracy. For the case study, the prediction accuracy is up to 92.64%. Besides, the proposed method is also real-time. It only takes approximately 0.5s to finish the seismic damage prediction of each ground motion.

(2) The deviations of the predicted seismic damage states can be controlled well. For the one-building case study, deviations among samples that are not correctly predicted are all limited within ±1 level. This characteristic further highlights the potential practical value of the proposed method.

(3) The complexity of the CNN networks should be moderate (such as Networks 3 and 4 in Table 2). The recommended dimension of the input figures for training CNN is 64 pixels × 64 pixels. The recommended range of learning rate is 0.005 to 0.01. The value of dropout ratio doesn’t have significant influence on this task.

The economic losses and casualties caused by earthquakes are closely related to the damage states of the target building or region. Therefore, on condition that the damage state is acquired through the proposed method, further loss and casualty assessments are feasible based on existing methods (e.g., [43, 44]).

6. Acknowledgements

The authors are grateful for the financial support received from the National Natural Science Foundation of China (No. U1709212) and the Tsinghua Scholarship for Overseas Graduate Studies which supports Yongjia Xu's visit to the University of California, Los Angeles (under the guidance of Prof. Ertugrul Taciroglu).

7. References

[1] China News Service (2008): The number of deaths in Mianyang city due to the earthquake was nearly 16,000, available at http://www.chinanews.com/gn/news/2008/05-21/1256776.shtml (last accessed 1 January, 2020). (In Chinese)
[2] Wald DJ, Jaiswal K, Marano KD, Bausch D, Hearne M (2010): Pager - rapid assessment of an earthquake's impact. *Fact Sheet*, Center for Integrated Data Analytics Wisconsin Science Center, 2010-3036.
[3] European Commission (2020): Global disaster alert and coordination system (GDACS) available at http://www.gdacs.org/ (last accessed 1 January, 2020).
[4] Lu XZ, Guan H (2017): *Earthquake Disaster Simulation of Civil Infrastructures: From Tall Buildings to Urban Areas*. Springer.
[5] Lu XZ, Cheng QL, Xu Z, Xu YJ, Sun CJ (2019): Real-time city-scale time-history analysis and its application in resilience-oriented earthquake emergency responses. *Applied Sciences*, **9** (17): 3497.
[6] Xiong C, Lu XZ, Lin XC, Xu Z, Ye LP (2017): Parameter determination and damage assessment for THA-based regional seismic damage prediction of multi-story buildings. *Journal of Earthquake Engineering*, **21** (3), 461-485.
[7] Xiong C, Lu XZ, Huang J, Guan H (2019): Multi-LOD seismic-damage simulation of urban buildings and case study in Beijing CBD. *Bulletin of Earthquake Engineering*, **17** (4), 2037-2057.
[8] Mahin S, Deierlein G, Govindjee S, Lowes L, Kareem A, Crittenden C, McKenna F, Schoettler M (2018): SimCenter computational framework for simulating and mitigating the effects of earthquakes. *Proceedings of the 11th Earthquake Engineering National Conference*, 25-29 June, 2018, Los Angeles, USA.
[9] Yu E, Taciroglu E, Wallace JW (2007): Parameter identification of framed structures using an improved finite element model updating method, Part I: Formulation & verification. *Earthquake Engineering & Structural Dynamics*, **36**, 619-639.
[10] Taciroglu E, Ghahari SF, Abazarsa F (2017): Efficient model updating of a multi-story frame and its foundation stiffness from earthquake records using a Timoshenko beam model. *Soil Dynamics and Earthquake Engineering*, **92**, 25-35.
[11] Hori M (2011). *Introduction to Computational Earthquake Engineering*, Imperial College Press, 2nd edition.
[12] Giovenale P, Cornell CA, Esteva L (2004): Comparing the adequacy of alternative ground motion intensity measures for the estimation of structural responses. *Earthquake Engineering & Structural Dynamics*, **33** (8), 951-979.
[13] Baker JW, Cornell CA (2008): Vector-valued intensity measures incorporating spectral shape for prediction of structural response. *Journal of Earthquake Engineering*, **12** (4), 534-554.
[14] Gehl P, Seyedi DM, Douglas J (2013): Vector-valued fragility functions for seismic risk evaluation. *Bulletin of Earthquake Engineering*, **11** (2), 365-384.
[15] Zareian F, Kaviani P, Taciroglu E (2015). Multi-phase performance assessment of seismic response of structures. *ASCE Journal of Structural Engineering*, **141** (11): 04015041.
[16] Boashash B (2003): *Time-Frequency Signal Analysis and Processing: A Comprehensive Reference*. Academic Press.
[17] Bradford SC (2006): *Time-Frequency Analysis of Systems with Changing Dynamic Properties*. Ph.D. Thesis, California Institute of Technology, Pasadena CA.
[18] Abazarsa F, Nateghi F, Ghahari SF, Taciroglu E (2016): Identification technique for non-stationary excitations and its verification and validation. *ASCE Journal of Engineering Mechanics*, **142** (2), 04015078: 1-19.
[19] Daubechies I (1990): The wavelet transform, time-frequency localization and signal analysis. *IEEE Transactions on Information Theory*, **36** (5), 961-1005.

[20] Salehi H, Burgueno R (2018): Emerging artificial intelligence methods in structural engineering. *Engineering Structures*, **171**, 170-189.
[21] Vetrivel A, Gerke M, Kerle N, Nex F, Vosselman G (2018): Disaster damage detection through synergistic use of deep learning and 3D point cloud features derived from very high resolution oblique aerial images, and multiple-kernel-learning. *ISPRS Journal of Photogrammetry and Remote Sensing*, **140**, 45-59.
[22] Xiong C, Li QS, Lu XZ (2020): Automated regional seismic damage assessment of buildings using an unmanned aerial vehicle and a convolutional neural network. *Automation in Construction*, **109**, 102994.
[23] PEER (2020): PEER NGA database (NGA-West, NGA-West2, NGA-East), available at https://peer.berkeley.edu/research/data-sciences (last accessed 1 January, 2020).
[24] NIED (2020): The NIED strong-motion seismograph networks, available at http://www.kyoshin.bosai.go.jp (last accessed 1 January, 2020).
[25] FEMA (2012): *Multi-Hazard Loss Estimation Methodology: Earthquake Model (HAZUS-MH 2.1 Technical Manual)*. Tech. Rep., Washington, D.C.
[26] China Earthquake Administration (CEA) (2009): *Classification of Earthquake Damage to Buildings and Special Structures (GB/T 24335-2009)*. Standards Press of China. (In Chinese)
[27] Yang C, Guo K, Zhang SL, Huang ZB (2015): Status quo of China earthquake networks and analysis on its early warning capacity. *Acta Seismologica Sinica*, **37**(3), 508-515. (In Chinese)
[28] Bommer JJ, Acevedo AB (2004): The use of real earthquake accelerograms as input to dynamic analysis. *Journal of Earthquake Engineering*, **8** (spec01), 43-91.
[29] Watson-Lamprey J, Abrahamson N (2006): Selection of ground motion time series and limits on scaling. *Soil Dynamics & Earthquake Engineering*, **26** (5), 477-482.
[30] Luco N, Bazzurro P (2007): Does amplitude scaling of ground motion records result in biased nonlinear structural drift responses. *Earthquake Engineering & Structural Dynamics*, **36** (13), 1813-1835.
[31] Goel RK, Chopra A (1997): Period formulas for moment-resisting frame buildings. *ASCE Journal of Structural Engineering*, **123** (11), 1454-1461.
[32] Ministry of Housing and Urban-Rural Development of the People's Republic of China (MOHURD) (2010): *Code for Seismic Design of Buildings (GB 50011-2010)*. China Architecture & Building Press. (In Chinese)
[33] PyWavelets (2019): PyWavelets - wavelet transforms in Python, software, https://pywavelets.readthedocs.io/en/latest/.
[34] Liu PC, Archuleta RJ, Hartzell SH (2006): Prediction of broadband ground-motion time histories: Hybrid low/high-frequency method with correlated random source parameters. *Bulletin of the Seismological Society of America*, **96** (6), 2118-2130.
[35] Mai PM, Dalguer LA (2012): Physics-based broadband ground-motion simulations: rupture dynamics combined with seismic scattering and numerical simulations in a heterogeneous earth crust. *Proceedings of the 15th Earthquake Engineering World Conference*, 24-28, Lisbon, Portugal.
[36] Wikipedia (2020): Convolutional neural network, available at https://en.wikipedia.org/wiki/Convolutional_neural_network (last accessed 1 January, 2020).
[37] TensorFlow (2020): TensorFlow API, available at https://www.tensorflow.org/api_docs/python (last accessed 1 January, 2020).
[38] Abadi M, Agarwal A, Barham P, Brevdo E, Chen ZF, Citro C, ..., Ghemawat S (2016): Tensorflow: Large-scale machine learning on heterogeneous distributed systems. Software available from tensorflow.org.
[39] Sutskever I, Martens J, Dahl G, Hinton G (2013): On the importance of initialization and momentum in deep learning. *Proceedings of International Conference on Machine Learning*, Atlanta, USA.
[40] Wikipedia (2020): Cross entropy, available at https://en.wikipedia.org/wiki/Cross_entropy (last accessed 1 January, 2020)
[41] Schmidhuber J (2015): Deep learning in neural networks: An overview. *Neural Networks*, **61**, 85-117.
[42] Srivastava N, Hinton G, Krizhevsky A, Sutskever I, Salakhutdinov R (2014): Dropout: a simple way to prevent neural networks from overfitting. *The Journal of Machine Learning Research*, **15** (1), 1929-1958.
[43] Zeng X, Lu XZ, Yang TY, Xu Z (2016): Application of the FEMA-P58 methodology for regional earthquake loss prediction. *Natural Hazards*, **83** (1), 177-192.
[44] Xu Z, Zhang HZ, Lu XZ, Xu YJ, Zhang ZC, Li Y (2019). A prediction method of building seismic loss based on BIM and FEMA P-58. *Automation in Construction*, **102**, 245-257.

